

The astrocyte-expressed integrin $\alpha v\beta 8$ governs blood vessel sprouting in the developing retina

Shinya Hirota^{1,*}, Qian Liu¹, Hye Shin Lee¹, Mohammad G. Hossain¹, Adam Lacy-Hulbert² and Joseph H. McCarty^{1,†}

SUMMARY

The mouse retina is vascularized after birth when angiogenic blood vessels grow and sprout along a pre-formed latticework of astrocytes. How astrocyte-derived cues control patterns of blood vessel growth and sprouting, however, remains enigmatic. Here, we have used molecular genetic strategies in mice to demonstrate that $\alpha v\beta 8$ integrin expressed in astrocytes is essential for neovascularization of the developing retina. Selective ablation of αv or $\beta 8$ integrin gene expression in astrocytes leads to impaired blood vessel sprouting and intraretinal hemorrhage, particularly during formation of the secondary vascular plexus. These pathologies correlate, in part, with diminished $\alpha v\beta 8$ integrin-mediated activation of extracellular matrix-bound latent transforming growth factor β s (TGF β s) and defective TGF β signaling in vascular endothelial cells, but not astrocytes. Collectively, our data demonstrate that $\alpha v\beta 8$ integrin is a component of a paracrine signaling axis that links astrocytes to blood vessels and is essential for proper regulation of retinal angiogenesis.

KEY WORDS: Extracellular matrix, Itgb8, Cell adhesion, Blood-retinal barrier, Angiogenesis, Mouse

INTRODUCTION

Neovascularization of the mouse retina initiates in the early neonatal period when endothelial cells and pericytes proliferate and migrate along astrocytes to form a primary vascular plexus. Blood vessels subsequently sprout into deeper retinal layers to form a secondary vascular network (Dorrell and Friedlander, 2006; Fruttiger, 2007). Various growth factors and cell-cell adhesion molecules such as platelet-derived growth factor (PDGF)-BB (Benjamin et al., 1998), vascular endothelial growth factor (VEGF)-A (Ruhberg et al., 2002; Gerhardt et al., 2003), Wnts (Phng et al., 2009) and Notch1-Dll4 (Hellstrom et al., 2007; Benedito et al., 2009) have been reported to play endothelial cell-intrinsic roles in retinal angiogenesis. Roles for astrocyte-derived factors in the regulation of retinal angiogenesis, and particularly those involving extracellular matrix (ECM) proteins and their cell adhesion receptors, remain largely uncharacterized.

Integrins are receptors for many ECM protein ligands (Silva et al., 2008), and integrin-mediated adhesion and signaling events are essential for blood vessel development and physiology in all mammalian organs, including the retina (Ramjaun and Hodivala-Dilke, 2009). For example, the laminin receptor $\alpha 3\beta 1$ integrin is expressed in vascular endothelial cells and acts to suppress pathological angiogenesis in the retina and other organs (Watson et al., 2010). Similarly, $\alpha v\beta 3$ and $\alpha v\beta 5$ integrins expressed in vascular

endothelial cells negatively regulate hypoxia-induced retinal angiogenesis (Hodivala-Dilke et al., 1999; Reynolds et al., 2002). Fibronectin, which is expressed primarily by astrocytes in the retina, has been reported to signal via $\alpha 5\beta 1$ integrin to promote development of the primary vascular plexus (Stenzel et al., 2011). Lastly, TGF β s, which in their ECM-bound latent forms are protein ligands for some αv -containing integrins (Worthington et al., 2010), have also been reported to regulate retinal blood vessel physiology and homeostasis of the blood-retinal barrier (Walshe et al., 2009).

During embryonic development, the neuroepithelial cell-expressed integrin $\alpha v\beta 8$ is essential for cerebral angiogenesis and blood-brain barrier development. Genetic ablation of αv or $\beta 8$ integrin expression in the embryonic neuroepithelium, but not the vascular endothelium, leads to abnormal cerebral blood vessel patterning and severe intracerebral hemorrhage (McCarty et al., 2002; Zhu et al., 2002; McCarty et al., 2005; Proctor et al., 2005). $\alpha v\beta 8$ integrin binds to RGD peptide sequences within latent TGF $\beta 1$ and TGF $\beta 3$, mediating TGF β release from the ECM and subsequent receptor engagement and signaling (Cambier et al., 2005; Mu et al., 2008). Indeed, endothelial cell-specific ablation of TGF β receptors results in brain vascular pathologies during embryogenesis that are strikingly similar to those that develop in $\alpha v\beta 8$ integrin and TGF β mutant embryos (Nguyen et al., 2011).

Here, functions for $\alpha v\beta 8$ integrin during physiological angiogenesis in the retina have been investigated. We show that genetic ablation of $\alpha v\beta 8$ integrin in astrocytes, and particularly during formation of the secondary vascular plexus, leads to defective retinal blood vessel sprouting and severe intraretinal hemorrhage. These data highlight that $\alpha v\beta 8$ integrin is an essential paracrine regulator of angiogenesis in the developing retina.

MATERIALS AND METHODS

Experimental mice

$\beta 8^{+/-}$ and $\beta 8^{flox/flox}$ mice were obtained from the Mutant Mouse Regional Resource Center. Genotypes were determined using PCR-based methodologies as previously described (Zhu et al., 2002; Proctor et al., 2005). Nestin-Cre transgenic mice (Tronche et al., 1999) were purchased

¹Department of Cancer Biology, University of Texas MD Anderson Cancer Center, Houston, TX 77030, USA. ²Department of Pediatrics, Massachusetts General Hospital, Boston, MA 02114, USA.

*Present address: Department of Human and Engineered Environmental Studies, University of Tokyo, Tokyo, Japan

†Author for correspondence (jhmccarty@mdanderson.org)

This is an Open Access article distributed under the terms of the Creative Commons Attribution Non-Commercial Share Alike License (<http://creativecommons.org/licenses/by-nc-sa/3.0/>), which permits unrestricted non-commercial use, distribution and reproduction in any medium provided that the original work is properly cited and all further distributions of the work or adaptation are subject to the same Creative Commons License terms.

from Jackson Laboratories. To generate control and $\beta 8$ integrin conditional knockout mice, females harboring a floxed $\beta 8$ integrin gene ($\beta 8^{\text{flox/flox}}$) were bred with hemizygous Nestin-Cre ($N\text{-Cre}^{+/-}$) transgenic males. Genotypes of F1 progeny were determined by PCR-based amplification of genomic DNA isolated from tail snips (Proctor et al., 2005). $N\text{-Cre}^{+/-};\beta 8^{\text{flox/+}}$ males were then crossed with $\beta 8^{\text{flox/flox}}$ females. Controls ($N\text{-Cre}^{+/-};\beta 8^{\text{flox/+}}$) were heterozygous null for $\beta 8$ integrin gene expression in cells that express Cre, whereas mutant littermates ($N\text{-Cre}^{+/-};\beta 8^{\text{flox/flox}}$) were homozygous null for $\beta 8$ integrin gene expression in Cre-expressing cells. Generation of $N\text{-Cre};\alpha v^{\text{flox/flox}}$ mice has been described previously (McCarty et al., 2005). Mice harboring the $Tgfb2^{\text{flox/flox}}$ gene were kindly provided by Dr Jonathan Currie (University of Texas M. D. Anderson Cancer Center, TX, USA) and have been described elsewhere (Chytil et al., 2002). To generate $Tgfb2$ conditional knockout mice, $N\text{-Cre}^{+/-}$ males were bred with $Tgfb2^{\text{flox/flox}}$ females. $N\text{-Cre}^{+/-};Tgfb2^{\text{flox/+}}$ males were then bred with $Tgfb2^{\text{flox/flox}}$ females to generate control and mutant littermates. Mice were genotyped using the following primers: 5'-TAAACAAGGTCCGGAGCCCA-3' and 5'-ACTTCTGCAAGAGTCCCT-3'. Genotyping of GFAP-CreERT2 transgenic mice has been described elsewhere (Hirrlinger et al., 2006).

GFAP-CreERT2 $^{+/-};\beta 8^{+/-}$ males were bred with $\beta 8^{\text{f/f}}$ females to generate control and mutant F1 progeny. Alternatively, GFAP-CreERT2 $^{+/-}$ males were bred with Rosa26:lox-STOP-lox-YFP females. P1 neonates were injected intragastrically with 50 μl tamoxifen (Sigma) prepared in sterile sunflower oil (1 mg/ml) once per day for three consecutive days as described previously (Pitulescu et al., 2010). Control and mutant cohorts were sacrificed ten days after the last injection and eyes were fixed for 24 hours in 4% paraformaldehyde (PFA) in PBS. Whole retinas were isolated and then analyzed by immunofluorescence staining using anti-CD31 and anti-GFAP monoclonal antibodies or anti-GFP rabbit polyclonal antibody, which cross-reacts with YFP (Abcam).

Isolation of primary retinal astrocytes

Astrocytes were cultured from P5 neonatal retinas and grown on laminin-coated dishes. Briefly, eyes were removed and placed in ice-cold Hank's Balanced Salt Solution (HBSS). Retinal cups were dissected and digested for 30 minutes at 37°C in DMEM containing 100 U/ml collagenase (Worthington) and 40 $\mu\text{g}/\text{ml}$ DNAase (Sigma). The tissue was then triturated and the single-cell suspension was plated onto T-25 tissue culture flasks pre-coated with mouse 3 $\mu\text{g}/\text{ml}$ laminin (Sigma). After 7 days, confluent cultures were placed on a rotary shaker overnight (250 rpm) to remove contaminating cells. Astrocyte genotypes were confirmed by genomic PCR using primers specific for the $\beta 8$ integrin gene (Jung et al., 2010). Retinal astrocytes were serum-starved for 18 hours and conditioned media was pre-treated with anti-TGF β antibodies (R&D Systems) or control IgGs (both at 5 $\mu\text{g}/\text{ml}$) for one hour. Conditioned media was then added to semi-confluent monolayers of bovine brain microvascular endothelial cells (Lonza). Cells were lysed in RIPA buffer and then immunoblotted with anti- β -actin (Sigma) or anti-pSmad3 rabbit antibodies (Epitomics).

Immunoblotting and immunofluorescence

Cells and tissues were lysed in RIPA buffer (10 mM Tris, pH 7.4, 1% NP40, 0.5% deoxycholate, 0.1% SDS, 150 mM NaCl and 1 mM EDTA). Protein concentrations in detergent-soluble fractions were determined using a BCA assay kit (Thermo Scientific) prior to incubation with primary and secondary antibodies. Secondary antibodies used for fluorescence were Alexa-conjugated goat anti-rabbit and goat anti-mouse (Molecular Probes). The following commercially antibodies were used for immunofluorescence: anti-GFAP rabbit polyclonal (DAKO); anti-GFAP mouse monoclonal (Millipore); anti-CD31 rat monoclonal (Pharmingen); anti-NG2 (Millipore); anti-pH3 (Cell Signaling), anti-GFP (Abcam) and anti-laminin (Sigma). The anti- αv and anti- $\beta 8$ integrin rabbit polyclonal antibodies have been described elsewhere (Tchaicha et al., 2010; Tchaicha et al., 2011).

Whole-mount retinal analysis

Neonatal mice were sacrificed and eyes were removed and fixed in 4% PFA in PBS at 4°C for 12 hours. Whole retinal cups were then microdissected, blocked in 1% bovine serum albumin (BSA) with 0.1%

Triton X-100 in PBS and incubated in primary antibodies for 16 hours at 4°C. Tissues were then washed five times in PBS at room temperature and then incubated overnight in secondary antibodies. Washed retinal cups were then flat-mounted on microscope slides.

Quantitation of retinal defects

To quantify numbers of filopodia per tip cell, randomly selected micrograph images ($n=3$ images per retina, $n=3$ mice per genotype) were analyzed at 400 \times magnification. Individual tip cells (>25 cells per genotype) were identified at the leading edge of the P5 vascular front and CD31-expressing filopodia were counted. Alternatively, to quantify filopodia sprouts per vessel length NIH ImageJ software was used to count projects per 100 μm at the leading edge of the migrating vessel front ($n=3$ images per retina, $n=3$ mice per genotype). Student's *t*-test was performed to determine statistically significant differences between groups.

Intraocular injections of anti-TGF β antibodies

P9 neonatal mice were deeply anaesthetized by intraperitoneal injection with tribromoethanol (Sigma), and then injected intraocularly using a 10 μl Hamilton syringe. Pups were injected with 2 μl PBS, 2 μl anti-TGF β blocking antibody (1 mg/ml, R&D Systems) or 2 μl isotype control antibody ($n=5$ mice injected per condition). Six hours later, mice were sacrificed and eyes were fixed for 12 hours in 4% PFA in PBS. Whole retinal cups were then microdissected and incubated in IsoB4-Alexa488 (Sigma) for 16 hours at 4°C. Retinas were washed five times in PBS at room temperature and flat-mounted on microscope slides for analysis.

RESULTS

$\alpha v\beta 8$ integrin is expressed in the neonatal mouse retina and in cultured retinal astrocytes

Angiogenic blood vessels invade the retina along a pre-formed network of glial fibrillary associated protein (GFAP)-expressing astrocytes (Kubota and Suda, 2009). We interrogated $\alpha v\beta 8$ integrin expression in cultured retinal astrocytes from wild-type and $\beta 8^{-/-}$ mice. Primary cells were cultured from P5 wild-type and $\beta 8^{-/-}$ littermates ($n=3$ mice per genotype) and grown on laminin-coated dishes. Nearly 100% of cells from both control and mutant littermates expressed GFAP and showed similar in vitro morphologies (Fig. 1A,B), although $\beta 8^{-/-}$ cells showed impaired proliferation and survival in vitro (data not shown). Detergent-soluble lysates prepared from control and $\beta 8^{-/-}$ astrocytes were immunoblotted with anti- αv and anti- $\beta 8$ integrin antibodies. Robust levels of αv and $\beta 8$ integrin proteins were detected in lysates from wild-type retinal astrocytes, whereas $\beta 8$ integrin protein was absent in $\beta 8^{-/-}$ lysates owing to gene ablation (Fig. 1C). Continued expression of αv integrin protein was detected in $\beta 8^{-/-}$ lysates owing to expression of other αv -associated integrin subunits, such as $\beta 1$ and $\beta 5$ integrins (data not shown). Retinal lysates were also prepared from P3, P7 and P14 wild-type mice and immunoblotted with anti-integrin antibodies to reveal robust αv and $\beta 8$ integrin protein expression at all developmental ages analyzed (Fig. 1D).

Angiogenesis defects and intraretinal hemorrhage upon formation of the secondary vascular plexus in $\beta 8^{-/-}$ mice

Retinas from P5 wild-type and $\beta 8^{-/-}$ littermates ($n=7$ mice per genotype) were isolated and labeled with anti-CD31 and anti-NG2 antibodies to visualize vascular endothelial cells and pericytes, respectively. Endothelial tip cells within the wild-type primary vascular plexus extended elaborate filopodial projections (Fig. 2A), whereas in $\beta 8^{-/-}$ retinas endothelial tip cells displayed less elaborate and blunted morphologies (Fig. 2B). In both wild-type and $\beta 8^{-/-}$ retinas, endothelial cells were closely associated with

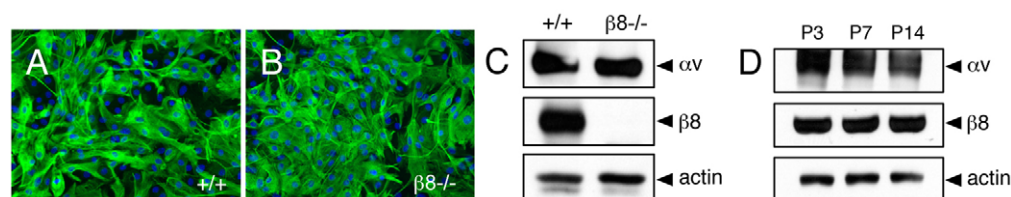


Fig. 1. α v β 8 integrin is expressed in mouse neonatal retinal astrocytes. (A,B) Retinal astrocytes were cultured from wild-type (A) or β 8 $^{-/-}$ (B) P5 littermates. Immunofluorescence reveals that the majority of cells (>95%) express GFAP. (C) Detergent-soluble astrocyte lysates were immunoblotted with anti- α v and anti- β 8 integrin antibodies. Note the robust α v β 8 integrin expression in wild-type cells, whereas there is complete loss of β 8 integrin protein expression in β 8 $^{-/-}$ cells owing to integrin gene ablation. (D) Detergent-soluble lysates were prepared from P3, P7 and P14 wild-type retinas and then immunoblotted with anti- α v and anti- β 8 integrin antibodies. Note the robust expression of α v and β 8 integrin proteins at the various developmental ages.

NG2-expressing pericytes, and no apparent differences in pericyte coverage were detected. Wild-type and β 8 $^{-/-}$ retinas from P5 littermates ($n=5$ mice per genotype) were also labeled with anti-CD31 and anti-GFAP antibodies to visualize vascular endothelial cells and astrocytes, respectively (Fig. 2C,D). Endothelial tip cell defects were detected in β 8 $^{-/-}$ retinas; however, no differences in the network of GFAP-expressing astrocytes were detected. We further analyzed tip cell defects in P5 wild-type and β 8 $^{-/-}$ retinas ($n=3$ retinas per genotype) by quantifying numbers of CD31-expressing filopodia per tip cell ($n \geq 25$ tip cells from three mice per genotype). As shown in Fig. 2E, a reduction of nearly 50% in numbers of filopodia per tip cell was detected in β 8 $^{-/-}$ retinas. We also detected reduced numbers of endothelial filopodia per defined vessel length at the leading edge of the migrating blood vessel network in β 8 $^{-/-}$ samples (Fig. 2F).

Beginning at \sim P8, blood vessels in the primary vascular plexus migrate along Müller glial cells into deeper retinal layers to form a secondary vascular network (Fruttiger, 2007). Analysis of retinas

from P12-14 wild-type or β 8 $^{-/-}$ mice ($n \geq 10$ per genotype) revealed grossly obvious intraretinal hemorrhage in 100% of mutants that was not present in any wild-type retinas analyzed (Fig. 3A). Anti-CD31 and anti-NG2 double immunofluorescence staining of wild-type P14 retinas ($n=5$ per genotype) revealed normal endothelial cell and pericyte interactions in vessels sprouting from the primary plexus into the underlying neuronal layers (Fig. 3B). Consistent with a marked defect in formation of a secondary vascular network, many capillaries within the primary vascular plexus of β 8 $^{-/-}$ mice failed to sprout into the deeper retinal layers and instead displayed glomeruloid-like tufts comprising both endothelial cells and pericytes (Fig. 3C). Double immunofluorescence staining with anti-CD31 and anti-GFAP was also performed to visualize interactions between endothelial cells and astrocytes. An elaborate astrocyte latticework was present in both wild-type and β 8 $^{-/-}$ samples (Fig. 3D,E), although increased GFAP expression was detected in mutant retinas probably owing to reactive gliosis in response to hemorrhage. Next, coronal sections from P12 wild-type and β 8 $^{-/-}$

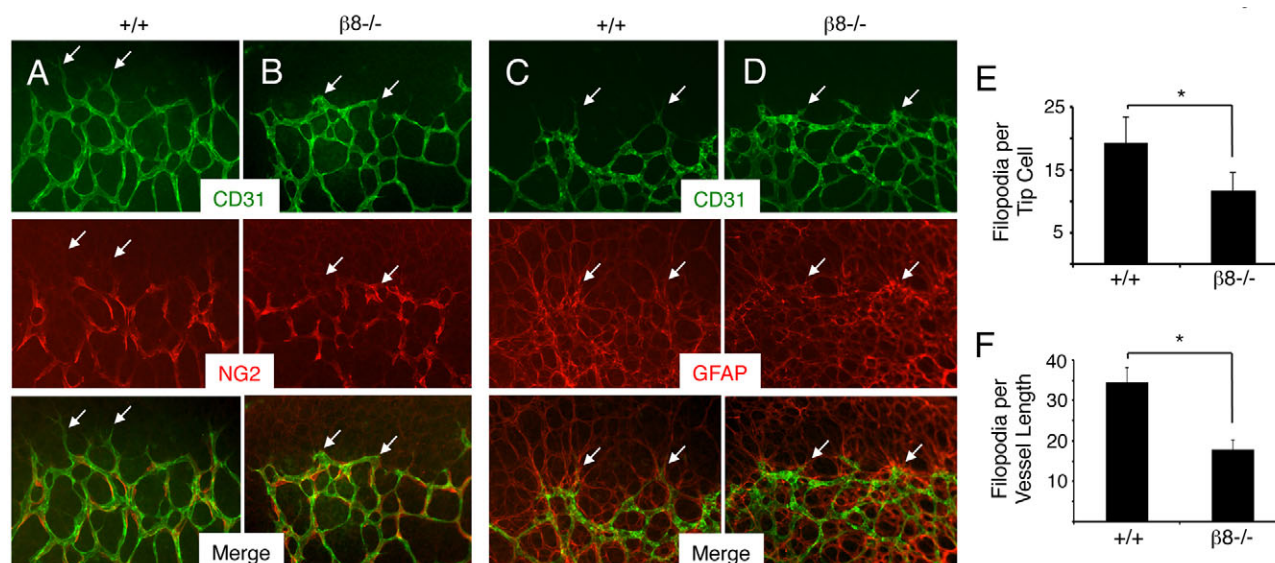


Fig. 2. β 8 $^{-/-}$ mice develop retinal vascular pathologies. (A,B) Retinas from P5 wild-type (A) or β 8 $^{-/-}$ (B) littermates were stained with anti-CD31 (green) and anti-NG2 (red) to visualize vascular endothelial cells and pericytes, respectively. Unlike the endothelial tip cells extending well-defined filopodia in wild-type retinas (arrows in A), note the blunted tip cell morphologies in β 8 $^{-/-}$ retinas (arrows in B). Note that endothelial cells are associated with pericytes in both control and β 8 $^{-/-}$ samples. (C,D) Retinas from P5 wild-type (C) or β 8 $^{-/-}$ (D) littermates were stained with anti-CD31 (green) and anti-GFAP (red) to visualize vascular endothelial cells and astrocytes, respectively. Note that endothelial cells in wild-type and β 8 $^{-/-}$ retinas are associated with a normal latticework of astrocytes. (E) Quantification of CD31 $^{+}$ filopodia per endothelial tip cell in retinas of wild-type and β 8 $^{-/-}$ mice. (F) Quantification of filopodial sprouts per 100 μ m retinal blood vessel length were quantified in wild-type and β 8 $^{-/-}$ mice. * $P < 0.001$. Error bars represent s.d. Images in A-D are shown at 200 \times magnification.

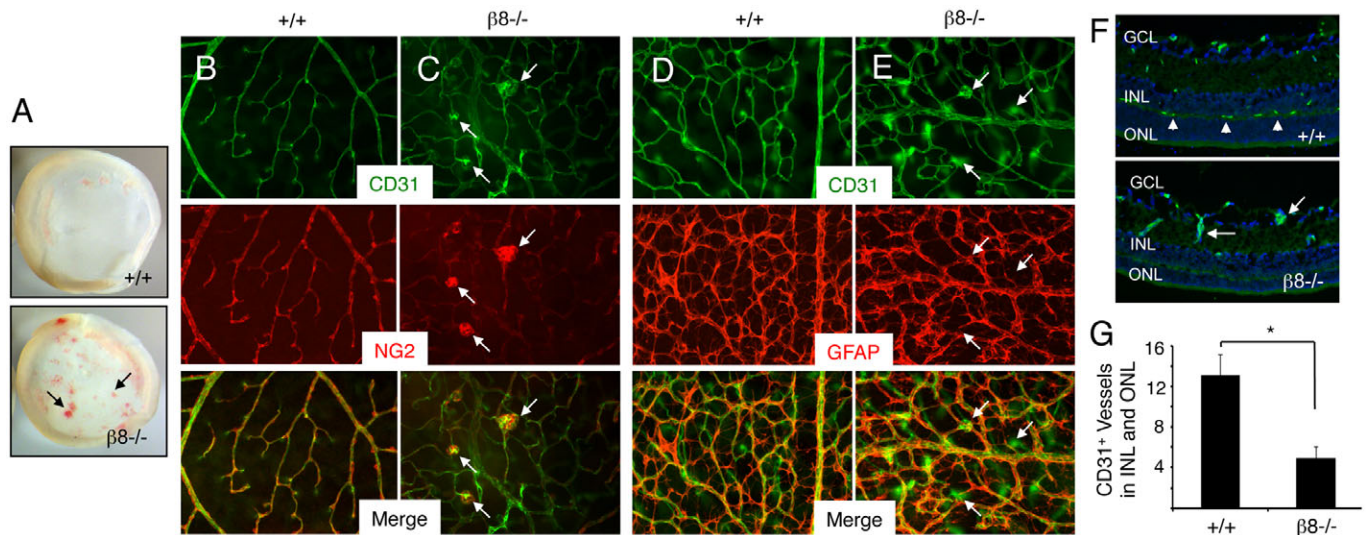


Fig. 3. Impaired development of the secondary retinal vascular plexus in $\beta 8^{-/-}$ mice. (A) Images of whole retinas isolated from P14 wild-type (upper panel) or $\beta 8^{-/-}$ (lower panel) littermates. Note the severe intraretinal hemorrhage in the $\beta 8^{-/-}$ sample (arrows). (B,C) Retinas from P14 wild-type (B) or $\beta 8^{-/-}$ (C) littermates were labeled with anti-CD31 and anti-NG2 antibodies to reveal vascular endothelial cells and pericytes, respectively. Note that in $\beta 8^{-/-}$ mice vascular endothelial cells display impaired sprouting into deeper retinal layers and form glomeruloid-like tufts that contain NG2-positive pericytes (arrows in C). (D,E) Retinas from P14 wild-type (D) or $\beta 8^{-/-}$ (E) littermates were labeled with anti-CD31 and anti-GFAP antibodies to reveal vascular endothelial cells and astrocytes, respectively. Although $\beta 8^{-/-}$ mice blood vessels form abnormal glomeruloid-like structures, the GFAP-expressing astrocyte network underlying the primary plexus appears normal (arrows in E). (F) Coronal sections through wild-type (upper panel) and $\beta 8^{-/-}$ (lower panel) retinas were stained with anti-CD31 to reveal vascular endothelial cells. Unlike the elaborate vascular sprouts in wild-type samples (arrowheads in upper panel), note the diminished blood vessel sprouting into the outer nuclear layer (ONL) and inner nuclear layer (INL) in $\beta 8^{-/-}$ mice (arrows in lower panel). GCL, ganglion cell layer. (G) Quantification of integrin-dependent formation of the secondary vascular plexus determined by quantifying blood vessels in the INL and ONL of wild-type and $\beta 8^{-/-}$ mice ($n=3$ sections per genotype). * $P<0.001$. Error bars represent s.d. Images in B-F are shown at 200 \times magnification.

retinas ($n=3$ mice per genotype) were immunostained with anti-CD31 antibodies. Wild-type sections contained blood vessels within all retinal layers; by contrast, fewer blood vessels were present in the inner nuclear layers and outer nuclear layers of $\beta 8^{-/-}$ retinal sections (Fig. 3F). Quantification of blood vessels within these layers in P12 wild-type and $\beta 8^{-/-}$ littermates ($n=3$ coronal sections per genotype) revealed significantly fewer blood vessels in $\beta 8^{-/-}$ samples (Fig. 3G).

The blunted blood vessel morphologies at P5 and tufted vascular structures at P14 suggested defects in endothelial cell proliferation and/or sprouting in $\beta 8^{-/-}$ retinas. To analyze integrin-dependent cell proliferation, we performed double immunofluorescence staining with antibodies directed against CD31 and phospho-histone H3 (pH3), which is phosphorylated at serine 28 in mitotic cells. As shown in supplementary material Fig. S1, no differences in numbers of pH3-expressing cells were detected in wild-type and $\beta 8^{-/-}$ samples at P5. Interestingly, the abnormal glomeruloid-like tufts at P14 did not contain elevated numbers of proliferating cells. These data indicate that the blood vessel defects in integrin mutants are likely to be due to impaired migration and sprouting but not proliferation.

Retinal blood vessel sprouting defects in mice lacking $\alpha v\beta 8$ integrin in astrocytes

$\beta 8$ integrin is reported to heterodimerize exclusively with the αv subunit (Nishimura et al., 1998); therefore, we analyzed functions for αv integrin in retinal astrocytes by selectively deleting a conditional αv integrin gene ($\alpha v\text{flox}/\text{flox}$) using Cre/lox strategies. Mice harboring a homozygous $\alpha v\text{flox}/\text{flox}$ gene (McCarty et al., 2005) were crossed to a Nestin-Cre transgenic strain that expresses Cre recombinase in neural progenitors and their astroglial and

neuronal progeny in the brain and retina (Tronche et al., 1999; Graus-Porta et al., 2001; Haigh et al., 2003). Nestin-Cre $^{+}/+;$ $\alpha v\text{flox}/+$ male progeny were then mated with $\alpha v\text{flox}/\text{flox}$ females to generate mutant progeny that were hemizygous for the Nestin-Cre transgene and homozygous for the αv integrin conditional gene (Nestin-Cre $^{+}/+;$ $\alpha v\text{flox}/\text{flox}$). Littermate controls were hemizygous for the Nestin-Cre transgene and carried one αv integrin flox allele and one wild-type allele (Nestin-Cre $^{+}/+;$ $\alpha v\text{flox}/+$).

As shown in Fig. 4A, PCR analysis of genomic DNA isolated from retinas of P14 Nestin-Cre $^{+}/+;$ $\alpha v\text{flox}/+$ mice confirmed Cre-mediated recombination of the $\alpha v\text{flox}$ allele. Immunoblotting of detergent-soluble retinal lysates prepared from Nestin-Cre $^{+}/+;$ $\alpha v\text{flox}/+$ control and Nestin-Cre $^{+}/+;$ $\alpha v\text{flox}/\text{flox}$ mutant littermates also revealed an obvious reduction in αv integrin protein levels in mutant retinas (Fig. 4B). Blood vessels in P5 control mice contained NG2-expressing pericytes and endothelial tip cells that extended multiple filopodia at the leading edge of the sprouting vascular network (supplementary material Fig. S2A). P5 mutant blood vessels contained NG2-expressing pericytes (supplementary material Fig. S2B); however, endothelial tip cells appeared blunted and displayed reduced numbers of filopodia in mutant samples (supplementary material Fig. S2E). No apparent differences in GFAP-expressing astrocytes were detected in P5 wild-type and $\beta 8^{-/-}$ retinas (supplementary material Fig. S2C,D).

Analysis of the retinal vasculature at P14, a time of robust angiogenesis in the secondary vascular plexus, revealed obvious intraretinal hemorrhage in αv conditional knockout mice (Fig. 4C). Nestin-Cre $^{+}/+;$ $\alpha v\text{flox}/\text{flox}$ retinas contained vessels with tufted morphologies comprising CD31-expressing cells and NG2-expressing pericytes (Fig. 4E). Increased GFAP expression was

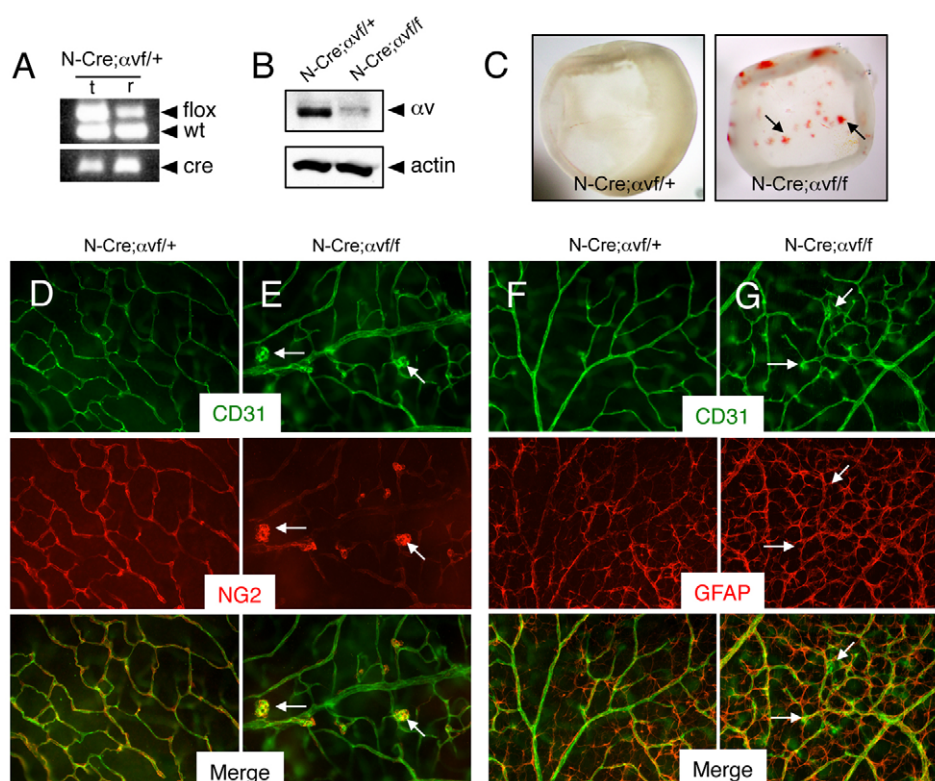


Fig. 4. Selective ablation of αv integrin gene expression in astrocytes causes retinal angiogenesis pathologies. (A) Confirmation of Nestin-Cre-mediated deletion of αv gene in P14 retinas (r) but not matched tail snips (t). Genomic DNA was analyzed by PCR-based methods. Note that in the retinal sample there is a reduction in the ~350 bp band owing to Cre-mediated recombination of the αv allele. (B) Detergent-soluble retinal lysates from P14 Nestin-Cre; αv lox/+ control or Nestin-Cre; αv lox/flox mice were immunoblotted with anti- αv antibodies. Note the diminished levels of αv integrin protein in mutant samples. (C) Images of retinas isolated from P14 Nestin-Cre; αv lox/+ control (left panel) or Nestin-Cre; αv lox/flox mutant mice (right panel) revealing intraretinal hemorrhage in mutant samples (arrows). (D,E) Retinas from P14 Nestin-Cre; αv lox/+ control (D) or Nestin-Cre; αv lox/flox mutant (E) mice were immunolabeled with anti-CD31 and anti-NG2 antibodies to visualize vascular endothelial cells and pericytes, respectively. Note the abnormal glomeruloid-like blood vessels comprising endothelial cells and pericytes in mutant samples (arrows in E). (F,G) Retinas from P14 Nestin-Cre; αv lox/+ control (F) or Nestin-Cre; αv lox/flox mutant (G) mice were immunolabeled with anti-CD31 and anti-GFAP antibodies to visualize vascular endothelial cells and astrocytes, respectively. Note that the abnormal vascular structures in mutant retinas (arrows in G) are associated with an apparently normal astrocyte network, although there is increased GFAP expression probably due to reactive astrogliosis resulting from intraretinal hemorrhage. Images in D-G are shown at 200 \times magnification.

apparent in mutant astrocytes, probably owing to reactive gliosis (Fig. 4F,G). These data, coupled with a previous report showing that deletion of αv integrin in vascular endothelial cells does not result in retinal angiogenesis defects (Lacy-Hulbert et al., 2007), further support essential functions for astrocyte-expressed αv integrins in retinal angiogenesis.

Next, mice harboring a homozygous $\beta 8$ lox/flox gene (Proctor et al., 2005) were crossed to a Nestin-Cre transgenic strain (Tronche et al., 1999). Nestin-Cre/+; $\beta 8$ lox/+ male progeny were then mated with $\beta 8$ lox/flox females to generate Nestin-Cre/+; $\beta 8$ lox/+ control and Nestin-Cre/+; $\beta 8$ lox/flox mutant progeny. PCR-based analysis using genomic DNA isolated from retinas of P14 Nestin-Cre/+; $\beta 8$ lox/+ mice confirmed Cre-mediated ablation of the $\beta 8$ lox allele (Fig. 5A). Retinal lysates from control and mutant littermates were immunoblotted with anti- $\beta 8$ integrin antibodies to reveal a reduction in $\beta 8$ integrin protein in mutant retinas (Fig. 5B). Blood vessels in P5 control retinas contained pericytes with endothelial tip cells extending multiple filopodia at the leading edge of the primary vascular plexus (supplementary material Fig. S3A). Differences in vessel-associated pericytes and GFAP-expressing astrocytes were not apparent in $\beta 8$ conditional knockouts (supplementary material Fig. S3B,D). However,

endothelial tip cells in P5 integrin mutants displayed blunted morphologies with reduced numbers of CD31-expressing filopodia (supplementary material Fig. S3E).

Analysis of the retinal vasculature at P14 revealed grossly obvious intraretinal hemorrhage in $\beta 8$ integrin conditional mutants, with many blood vessels in the primary plexus failing to sprout into the underlying retinal tissue (Fig. 5C; data not shown). Unlike controls (Fig. 5D), Nestin-Cre/+; $\beta 8$ lox/flox retinas contained vessels with abnormal branching patterns and glomeruloid-like tufts comprising CD31-expressing cells and NG2-expressing pericytes (Fig. 5E). Analysis of the retinal astrocyte network at P14 revealed reactive gliosis in mutants, probably owing to intraretinal hemorrhage (Fig. 5F,G). Collectively, these conditional knockout data further support essential roles for astrocyte-expressed $\alpha v\beta 8$ integrin in the control of neonatal retinal angiogenesis.

Inducible deletion of $\beta 8$ integrin in astrocytes leads to retinal angiogenesis pathologies

The Nestin-Cre transgene is expressed in embryonic neural progenitor cells that give rise to retinal astrocytes and neurons (Haigh et al., 2003) raising the possibility that loss of $\alpha v\beta 8$ integrin functions in astrocytes as well as neurons might contribute to

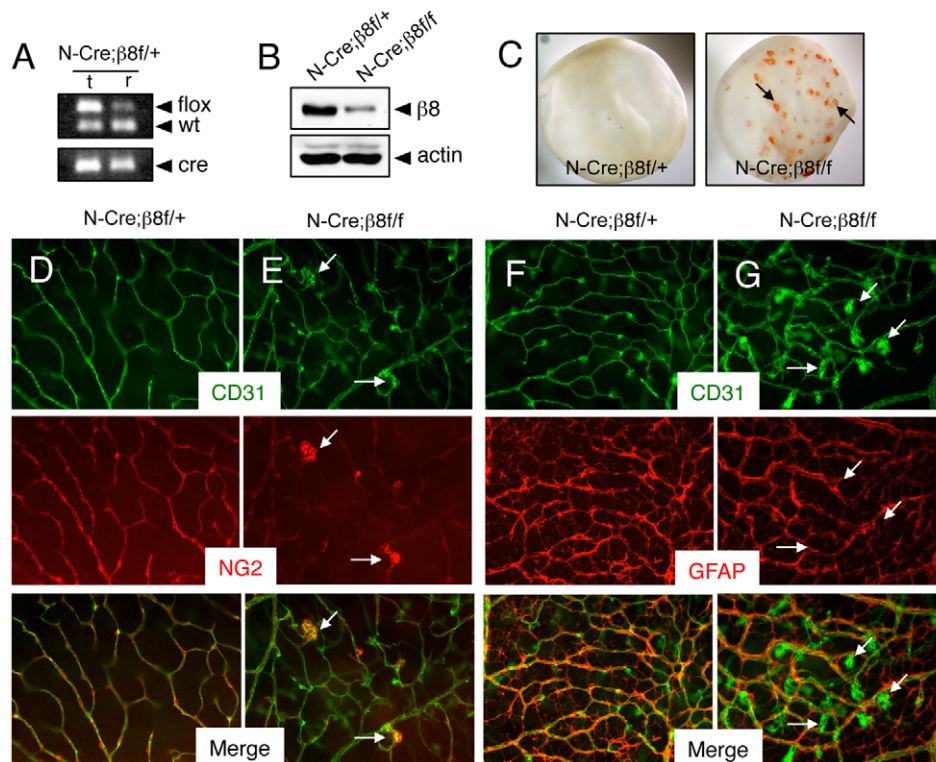


Fig. 5. Selective ablation of $\beta 8$ integrin gene expression in astrocytes causes retinal angiogenesis pathologies. (A) Nestin-Cre-mediated deletion of $\beta 8$ floxed gene in genomic DNA isolated from P14 retinas (r) but not in that isolated from matched tail snips (t). In the retina there is a reduction in the ~350 bp band owing to Cre-mediated recombination of the $\beta 8$ floxed allele. (B) Detergent-soluble retinal lysates from P14 Nestin-Cre; $\alpha\beta$ flox/+ control or Nestin-Cre; $\beta 8$ flox/flox mice were immunoblotted with anti- $\beta 8$ integrin antibodies. Note the diminished levels of $\beta 8$ integrin protein in mutant samples. (C) Images of retinas isolated from P14 Nestin-Cre; $\beta 8$ flox/+ control (left panel) or Nestin-Cre; $\beta 8$ flox/flox mutant mice (right panel) revealing intraretinal hemorrhage in mutant samples (arrows). (D,E) Retinas from P14 Nestin-Cre; $\beta 8$ flox/+ control (D) or Nestin-Cre; $\beta 8$ flox/flox mutant (E) mice were immunolabeled with anti-CD31 and anti-NG2 antibodies to visualize vascular endothelial cells and pericytes, respectively. Note the abnormal glomeruloid-like vascular tufts comprising endothelial cells and pericytes in mutant samples (arrows in E). (F,G) Retinas from P14 Nestin-Cre; $\beta 8$ flox/+ control (F) or Nestin-Cre; $\beta 8$ flox/flox mutant (G) mice were immunolabeled with anti-CD31 and anti-GFAP antibodies to visualize vascular endothelial cells and astrocytes, respectively. Note that the abnormal morphologies of blood vessels in conditional knockout retinas (arrows in G), although there is an apparently normal astrocyte latticework. Images in D-G are shown at 200 \times magnification.

retinal angiogenesis defects in integrin mutant mice. To study more selectively functions for $\alpha\beta 8$ integrin in astrocytes, we employed an inducible gene knockout strategy using a tamoxifen-responsive GFAP-CreERT2 transgene (Hirrlinger et al., 2006). First, to confirm tamoxifen-inducible activation of Cre we analyzed a Rosa26-lox-STOP-lox-YFP reporter strain. As shown in supplementary material Fig. S4A,B, mosaic patterns of Cre activity were detected in GFAP-expressing retinal astrocytes, but not in CD31-expressing endothelial cells.

GFAP-CreERT2/+; $\beta 8$ flox/+ male progeny were mated with $\beta 8$ flox/flox females to generate GFAP-CreERT2/+; $\beta 8$ flox/+ control and GFAP-CreERT2/+; $\beta 8$ flox/flox conditional mutants. To induce Cre activation, P1 pups were injected intragastrically with tamoxifen once per day for three consecutive days as previously described (Pitulescu et al., 2010). Ten days later, mice were sacrificed and retinas were analyzed for vascular pathologies and by immunofluorescent labeling with anti-CD31 antibodies. Analysis of P14 control and mutant animals ($n=4$ mice per genotype) revealed a lack of grossly obvious intraretinal hemorrhage. However, abnormal blood vessel morphologies within the primary vascular retinal plexus of GFAP-CreERT2/+; $\beta 8$ flox/flox inducible mutants were detected. In comparison with controls (supplementary material Fig. S4C), many

blood vessels in mutants formed tufted structures and failed to sprout into the underlying retinal cell layers (supplementary material Fig. S4D). In addition, blood vessels with tortuous morphologies were detected within cerebral cortices of mutant animals (supplementary material Fig. S5). The less severe vascular pathologies in the retinas of tamoxifen-inducible GFAP-CreERT2 mutants (as opposed to Nestin-Cre conditional mutants) might be due to more robust gene deletion patterns in nestin-expressing neural progenitor cells during embryonic development. Mosaic patterns of Cre activation in GFAP-CreERT2 transgenics probably results in heterogeneous loss $\beta 8$ integrin expression with many astrocytes expressing integrin protein. It also remains possible that $\beta 8$ integrin in retinal neurons as well as astrocytes determines patterns of neovascularization. Nonetheless, vascular pathologies in inducible knockout mice confirm that $\alpha\beta 8$ integrin in retinal astrocytes is essential for regulation of normal blood vessel sprouting in the developing retina.

Genetic ablation of TGF β signaling in astrocytes does not cause retinal angiogenesis pathologies

$\alpha\beta 8$ integrin is a receptor for latent TGF β and loss of integrin expression leads to diminished TGF β activation and signaling in the adult brain (Mobley et al., 2009; Su et al., 2010). Various

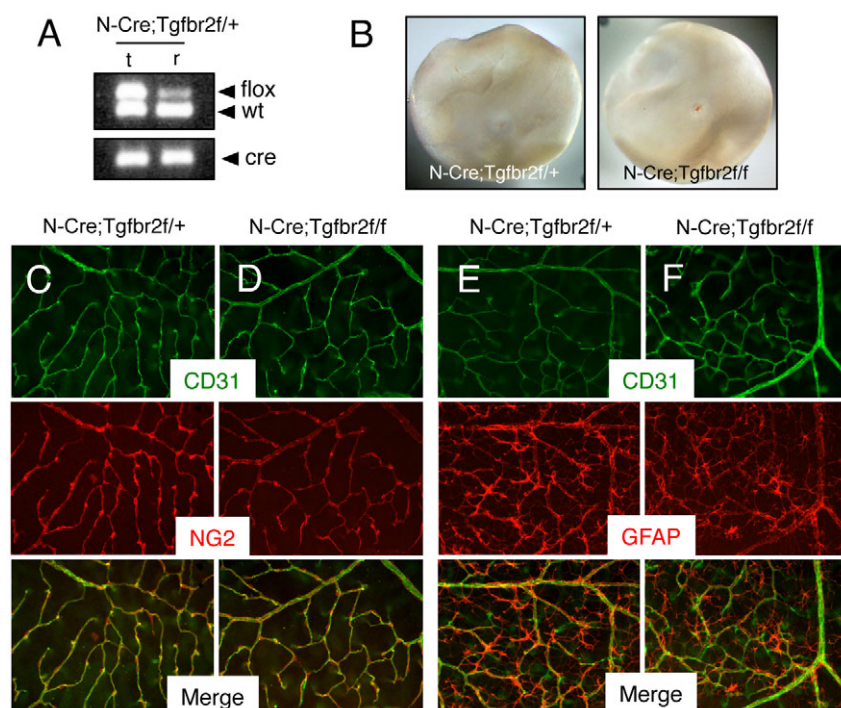


Fig. 6. Retinal angiogenesis is not perturbed in mice lacking *Tgfr2* gene expression in astrocytes.

(A) Nestin-Cre-mediated deletion of the *Tgfr2* floxed allele in genomic DNA isolated from the retina (r) but not matched tail snips (t) as confirmed by PCR analysis. In the retina there is a reduction in the ~500 bp band owing to Cre-mediated recombination of the *Tgfr2* floxed allele. (B) Images of retinas isolated from P14 Nestin-Cre;*Tgfr2* floxed/+ control (left panel) or Nestin-Cre;*Tgfr2* floxed/floxed mutant mice (right panel). Note the absence of hemorrhage in the mutant retinas. (C,D) Retinas from P14 control (C) and Nestin-Cre;*Tgfr2* floxed/floxed mutant (D) mice were immunolabeled with anti-CD31 and anti-NG2 antibodies to visualize vascular endothelial cells and pericytes, respectively. Note the normal blood vessel cytoarchitecture containing vascular endothelial cells and pericytes in control and mutant samples. (E,F) Retinas from P14 control (E) and Nestin-Cre;*Tgfr2* floxed/floxed mutant (F) mice were immunolabeled with anti-CD31 and anti-GFAP antibodies to visualize vascular endothelial cells and astrocytes, respectively. Note the normal endothelial cell and astrocyte interactions in both control and mutant samples. Images in C-F are shown at 200 \times magnification.

genetic studies have also linked α v β 8 integrin to TGF β s during embryonic brain development (Mu et al., 2008). To investigate a role for integrin-activated TGF β signaling in retinal neural cells, we selectively ablated expression of TGF β 2, which dimerizes with various type 1 TGF β receptors and is essential for the activation of intracellular signaling cascades (Massague and Gomis, 2006; Wu and Hill, 2009). Mice harboring a homozygous *Tgfr2* floxed/floxed gene (Chytil et al., 2002) were interbred with Nestin-Cre transgenic mice (Tronche et al., 1999). Nestin-Cre $^{+}$;*Tgfr2* floxed/+ male progeny were then mated with *Tgfr2* floxed/floxed females to generate mutant progeny that were hemizygous for the Nestin-Cre transgene and homozygous for the *Tgfr2* conditional allele.

Nestin-Cre $^{+}$;*Tgfr2* floxed/floxed conditional knockouts were born in the expected Mendelian ratios and displayed no obvious developmental phenotypes. Of 231 animals analyzed at P17, 55 mice (23%) were Nestin-Cre $^{+}$;*Tgfr2* floxed/floxed. Analysis of post-natal life span in control ($n=15$) and mutant ($n=13$) littermates reveal that *Tgfr2* mutants survive for up to two years without developing obvious phenotypes (Nguyen et al., 2011). For example, conditional knockout mice do not display neurological deficits resulting from blood-brain barrier breakdown (data not shown). These results are in contrast to adult α v and β 8 integrin mutant mice generated with Nestin-Cre, which develop progressive neurological deficits and die prematurely (McCarty et al., 2005; Proctor et al., 2005).

Retinas were isolated from P14 control and mutant mice, and Cre-mediated recombination of the *Tgfr2* floxed/floxed gene was confirmed by genomic PCR analysis (Fig. 6A). Unlike β 8 $^{-/-}$ mice (Fig. 1) or α v β 8 integrin conditional knockout mice generated with Nestin-Cre (Figs 4 and 5), intraretinal hemorrhage was not evident in Nestin-Cre;*Tgfr2* conditional mutants (Fig. 6B). Normal associations between endothelial cells, pericytes and retinal astrocytes were detected (Figs 6C-F) and the endothelial tip cell defects were not obvious (supplementary material Fig. S6). These

data reveal that ablation of TGF β receptor signaling in neural progenitor cells via Nestin-Cre does not negatively impact angiogenesis in the post-natal retina. Hence, α v β 8 integrin-dependent angiogenesis defects are not due to loss of autocrine TGF β signaling in retinal neural cells.

Retinal astrocytes signal to endothelial cells via TGF β s and intraocular injection of anti-TGF β blocking antibodies induces retinal angiogenesis pathologies

Recently, we reported the use of a novel Alk1-Cre knock-in mouse strain to investigate roles for TGF β 2 and Alk5 receptors in endothelial cells during embryonic brain angiogenesis (Nguyen et al., 2011). Mutant animals develop abnormalities in blood vessel patterning and intracerebral hemorrhage that phenocopies defects in mouse embryos lacking α v β 8 integrin in neuroepithelial cells (McCarty et al., 2005; Proctor et al., 2005). However, TGF β receptor mutant mice die during late stages of embryogenesis, which precludes analysis of TGF β signaling in retinal angiogenesis. Nonetheless, we hypothesized that the retinal angiogenesis pathologies in α v and β 8 integrin mutant mice were due to defective integrin-mediated TGF β activation and signaling to vascular endothelial cells.

To investigate paracrine TGF β signaling events between retinal astrocytes and endothelial cells, we performed in vitro cell culture experiments in which primary brain microvascular endothelial cells were treated with conditioned media taken from primary retinal astrocytes. As shown in Fig. 7A, a time-dependent increase in Smad3 phosphorylation was detected. Increased phosphorylation of Smad2 or Smad1/5/8 was not detected (data not shown). Smad3 phosphorylation was inhibited by pre-incubating conditioned medium with anti-TGF β neutralizing antibodies, but not control IgGs. These data reveal that retinal astrocytes produce active TGF β s that can signal to endothelial cells and activate intracellular pathways.

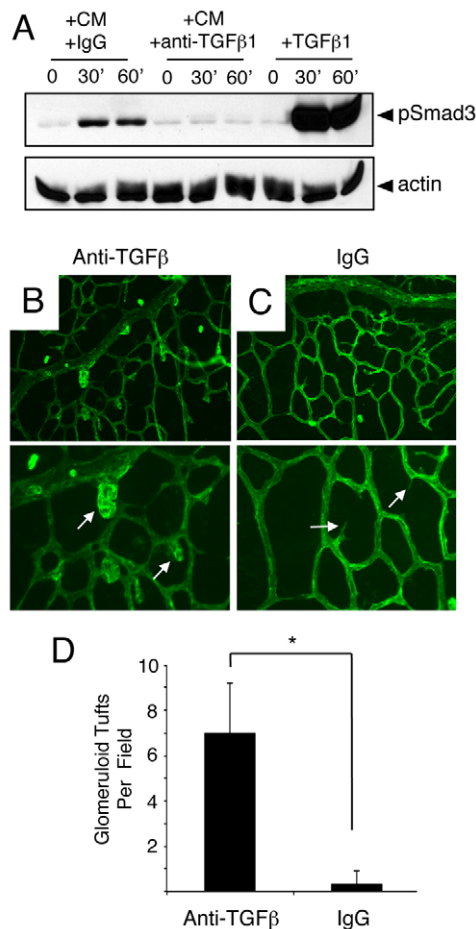


Fig. 7. Anti-TGF β neutralizing antibodies induce acute retinal angiogenesis defects. (A) Primary brain microvascular endothelial cells were treated for varying times (0, 30 or 60 minutes) with 1 ng/ml TGF β 1 (+TGF β) or retinal astrocyte conditioned media (CM) containing anti-TGF β neutralizing antibodies (+anti-TGF β) or control IgGs (+IgGs). Note that treatment of endothelial cell cultures with TGF β 1 or CM+IgG leads to a time-dependent increase in Smad3 phosphorylation. By contrast, anti-TGF β neutralizing antibodies inhibit Smad3 phosphorylation in endothelial cells. (B,C) P9 mouse pups were anesthetized and injected intraocularly with anti-TGF β neutralizing antibodies (B) or control IgGs (C). Retinas were fluorescently labeled with IsoB4-Alexa488 to visualize blood vessels. Note the abnormal blood vessel morphologies in P9 mice injected with anti-TGF β blocking antibodies (arrows in B). Images are shown at 200 \times magnification in the upper panels and at 400 \times magnification in lower panels. (D) Quantification of retinal angiogenesis pathologies in mice intraocularly injected with control IgGs or anti-TGF β antibodies. * $P < 0.001$. Error bars represent s.d.

Next, we used anti-TGF β neutralizing antibodies to analyze roles for TGF β signaling in retinal angiogenesis *in vivo*. P9 pups were anesthetized and injected intraocularly with control IgGs ($n=5$) or anti-TGF β antibodies ($n=5$) that we have shown previously block activation and signaling functions for all three TGF β family members (Mobley et al., 2009). Mice were sacrificed 6 hours after injection and blood vessel patterning was analyzed by staining whole retinas with IsoB4-Alexa488. Anti-TGF β blocking antibodies (Fig. 7B), but not control IgGs (Fig. 7C), induced acute defects in angiogenesis. Unlike intraocularly injected control IgGs,

anti-TGF β antibodies generated abnormal endothelial cell morphologies and the appearance of blood vessels with glomeruloid-like tufts. Quantification of retinal blood vessel pathologies revealed statistically significant more vascular tufts in mice injected intraocularly with anti-TGF β antibodies versus control IgGs (Fig. 7D).

DISCUSSION

In this report, we demonstrate functions for $\alpha v \beta 8$ integrin-mediated TGF β activation and signaling in neonatal retinal angiogenesis using a combination of cell type-specific gene knockout and signaling blockade strategies. Our experimental data reveal the following novel findings: (1) $\alpha v \beta 8$ integrin is expressed in retinal astrocytes (Fig. 1) and $\beta 8^{-/-}$ neonatal mice display blood vessel sprouting defects, particularly during formation of the secondary retinal vascular plexus (Figs 2 and 3); (2) selective ablation of αv or $\beta 8$ integrin gene expression in astrocytes via Nestin-Cre (Figs 4 and 5) or GFAP-CreERT2 (supplementary material Figs S4 and S5) leads to retinal vascular pathologies similar to those that develop in whole body $\beta 8^{-/-}$ mice; (3) genetic deletion of TGF β signaling in astrocytes does not lead to retinal vascular pathologies (Fig. 6); and (4) antibody-mediated inhibition of TGF β s leads to acute angiogenesis defects and impaired signaling events in endothelial cells (Fig. 7). Collectively, these data are the first to identify $\alpha v \beta 8$ integrin as an essential astrocyte-specific regulator of retinal angiogenesis.

Although we detect abnormalities in blood vessel spouting during formation of the primary vascular network, the most severe integrin-dependent pathologies occur upon development of the secondary retinal vascular plexus. Interestingly, the secondary plexus first forms when blood vessels migrate radially along GFAP-expressing Müller glia, which are morphologically similar to brain neuroepithelial cells (Zhang and Barres, 2010). The glomeruloid-like vascular tufts that develop in integrin mutants indicate that $\alpha v \beta 8$ integrin plays a crucial instructive role in promoting retinal blood vessel sprouting along Müller glia. The vascular tufts comprise both endothelial cells and pericytes, suggesting that integrin-expressing astrocytes might communicate with both cell types to induce proper patterns of radial sprouting.

How $\alpha v \beta 8$ integrin spatially controls endothelial cell and pericyte sprouting behaviors remains unclear, although local TGF β activation and signaling events are likely to be necessary. One possibility is that tip cells are enriched with TGF β receptors, which can bind to TGF β s activated locally by $\alpha v \beta 8$ integrin in perivascular astrocytes. In support of this model, Eichmann and colleagues have shown enrichment of TGF β receptors in endothelial tip cells of the primary retinal vascular plexus (del Toro et al., 2010). TGF β s might also bind to receptors in endothelial stalk cells or pericytes and regulate tip cell sprouting at the invading vascular front. Lastly, the retinal vascular phenotypes in integrin mutant mice might be due, in part, to defective astrocyte adhesion to ECM protein ligands other than latent TGF β s. $\alpha v \beta 8$ integrin has been identified as a receptor for vitronectin (Milner et al., 1997) as well as collagen IV and fibronectin (Venstrom and Reichardt, 1995); therefore, impaired signaling pathways regulated by these ECM proteins might contribute to the retinal vascular phenotypes.

It is enticing to speculate that integrin-activated TGF β s cooperatively signal with other growth factors to regulate blood vessel spouting. For example, perturbation of VEGF-A interactions with the ECM leads to impaired blood vessel morphogenesis in the retina (Ruhrberg et al., 2002), and these defects are similar to those

we report for integrin knockouts. However, inducible deletion of VEGF-A in astrocytes leads to only minor impairments in development of the primary and secondary vascular networks (Scott et al., 2010), revealing that other astrocyte-derived VEGF family members or other growth factors drive retinal neovascularization. One such factor is pigment epithelial-derived factor, which is expressed by Müller glia and is essential for blood vessel sprouting during formation of the secondary vascular plexus (Yafai et al., 2007). Astrocyte-expressed Norrin, a protein with structural similarities to TGFβs (Clevers, 2004) that signals via Frz4 and β-catenin, is also essential for formation of the secondary retinal vascular plexus (Xu et al., 2004; Ye et al., 2009). Norrin- and Frz4-deficient mice develop pathologies that phenocopy many of the retinal vascular defects that we report herein for αvβ8 integrin mutant mice. Hence, it is possible that integrin-activated TGFβ, Wnts and other adhesion pathways cooperatively control blood vessel sprouting in the developing retina.

Lastly, abnormal regulation of angiogenesis during retinal development is associated with retinopathy of prematurity, a vascular pathology that often leads to retinal detachment and blindness (Chen and Smith, 2007). It is likely that pathways involved in physiological retinal angiogenesis, including αvβ8 integrin activation of TGFβs, are altered in retinopathy of prematurity. Defining the signaling pathways that are differentially involved in neural versus vascular cells will be essential to understand better, and potentially treat, such diseases of development, as well as provide insight into how other CNS vascular pathologies might be prevented.

Acknowledgements

We are grateful to Dr Frank Kirchhoff (University of Saarland) for providing GFAP-CreERT2 transgenic mice and Dr Harold Moses (Vanderbilt University) for providing Tgfb2lox/flox mice.

Funding

This research was supported by grants from The Ellison Medical Foundation [AG-NS-0324-06 to J.H.M.] and the National Institutes of Neurological Disease and Stroke [R01NS059876 to J.H.M.]. Deposited in PMC for immediate release.

Competing interests statement

The authors declare no competing financial interests.

Supplementary material

Supplementary material available online at <http://dev.biologists.org/lookup/suppl/doi:10.1242/dev.069153/-DC1>

References

- Benedito, R., Roca, C., Sorensen, I., Adams, S., Gossler, A., Fruttiger, M. and Adams, R. H. (2009). The notch ligands Dll4 and Jagged1 have opposing effects on angiogenesis. *Cell* **137**, 1124-1135.
- Benjamin, L. E., Hemo, I. and Keshet, E. (1998). A plasticity window for blood vessel remodelling is defined by pericyte coverage of the preformed endothelial network and is regulated by PDGF-B and VEGF. *Development* **125**, 1591-1598.
- Cambier, S., Gline, S., Mu, D., Collins, R., Araya, J., Dolganov, G., Einheber, S., Boudreau, N. and Nishimura, S. L. (2005). Integrin alpha(v)beta8-mediated activation of transforming growth factor-beta by perivascular astrocytes: an angiogenic control switch. *Am. J. Pathol.* **166**, 1883-1894.
- Chen, J. and Smith, L. E. (2007). Retinopathy of prematurity. *Angiogenesis* **10**, 133-140.
- Chytil, A., Magnuson, M. A., Wright, C. V. and Moses, H. L. (2002). Conditional inactivation of the TGF-beta type II receptor using Cre:Lox. *Genesis* **32**, 73-75.
- Clevers, H. (2004). Wnt signaling: Ig-norrin the dogma. *Curr. Biol.* **14**, R436-R437.
- del Toro, R., Prahst, C., Mathivet, T., Siegfried, G., Kaminker, J. S., Larrievre, B., Breant, C., Duarte, A., Takakura, N., Fukamizu, A. et al. (2010). Identification and functional analysis of endothelial tip cell-enriched genes. *Blood* **116**, 4025-4033.
- Dorrell, M. I. and Friedlander, M. (2006). Mechanisms of endothelial cell guidance and vascular patterning in the developing mouse retina. *Prog. Retin. Eye Res.* **25**, 277-295.
- Fruttiger, M. (2007). Development of the retinal vasculature. *Angiogenesis* **10**, 77-88.
- Gerhardt, H., Golding, M., Fruttiger, M., Ruhrberg, C., Lundkvist, A., Abramsson, A., Jeltsch, M., Mitchell, C., Alitalo, K., Shima, D. et al. (2003). VEGF guides angiogenic sprouting utilizing endothelial tip cell filopodia. *J. Cell Biol.* **161**, 1163-1177.
- Graus-Porta, D., Blaess, S., Senften, M., Littlewood-Evans, A., Damsky, C., Huang, Z., Orban, P., Klein, R., Schittny, J. C. and Muller, U. (2001). Beta1-class integrins regulate the development of laminae and folia in the cerebral and cerebellar cortex. *Neuron* **31**, 367-379.
- Haigh, J. J., Morelli, P. I., Gerhardt, H., Haigh, K., Tsien, J., Damert, A., Miquelot, L., Muhlner, U., Klein, R., Ferrara, N. et al. (2003). Cortical and retinal defects caused by dosage-dependent reductions in VEGF-A paracrine signaling. *Dev. Biol.* **262**, 225-241.
- Hellstrom, M., Phng, L. K. and Gerhardt, H. (2007). VEGF and Notch signaling: the yin and yang of angiogenic sprouting. *Cell Adhes. Migr.* **1**, 133-136.
- Hirrlinger, P. G., Scheller, A., Braun, C., Hirrlinger, J. and Kirchhoff, F. (2006). Temporal control of gene recombination in astrocytes by transgenic expression of the tamoxifen-inducible DNA recombinase variant CreERT2. *Glia* **54**, 11-20.
- Hodivala-Dilke, K. M., McHugh, K. P., Tsakiris, D. A., Rayburn, H., Crowley, D., Ullman-Cullere, M., Ross, F. P., Collier, B. S., Teitelbaum, S. and Hynes, R. O. (1999). Beta3-integrin-deficient mice are a model for Glanzmann thrombasthenia showing placental defects and reduced survival. *J. Clin. Invest.* **103**, 229-238.
- Jung, Y., Kissil, J. L. and McCarty, J. H. (2010). beta8 integrin and band 4.1B cooperatively regulate morphogenesis of the embryonic heart. *Dev. Dyn.* **240**, 271-277.
- Kubota, Y. and Suda, T. (2009). Feedback mechanism between blood vessels and astrocytes in retinal vascular development. *Trends Cardiovasc. Med.* **19**, 38-43.
- Lacy-Hulbert, A., Smith, A. M., Tissire, H., Barry, M., Crowley, D., Bronson, R. T., Roes, J. T., Savill, J. S. and Hynes, R. O. (2007). Ulcerative colitis and autoimmunity induced by loss of myeloid alphav integrins. *Proc. Natl. Acad. Sci. USA* **104**, 15823-15828.
- Massague, J. and Gomis, R. R. (2006). The logic of TGFbeta signaling. *FEBS Lett.* **580**, 2811-2820.
- McCarty, J. H., Monahan-Earley, R. A., Brown, L. F., Keller, M., Gerhardt, H., Rubin, K., Shani, M., Dvorak, H. F., Wolburg, H., Bader, B. L. et al. (2002). Defective associations between blood vessels and brain parenchyma lead to cerebral hemorrhage in mice lacking alphav integrins. *Mol. Cell. Biol.* **22**, 7667-7677.
- McCarty, J. H., Lacy-Hulbert, A., Charest, A., Bronson, R. T., Crowley, D., Housman, D., Savill, J., Roes, J. and Hynes, R. O. (2005). Selective ablation of alphav integrins in the central nervous system leads to cerebral hemorrhage, seizures, axonal degeneration and premature death. *Development* **132**, 165-176.
- Milner, R., Frost, E., Nishimura, S., Delcommenne, M., Streuli, C., Pytela, R. and French-Constant, C. (1997). Expression of alphavbeta3 and alphavbeta8 integrins during oligodendrocyte precursor differentiation in the presence and absence of axons. *Glia* **21**, 350-360.
- Mobley, A. K., Tchaicha, J. H., Shin, J., Hossain, M. G. and McCarty, J. H. (2009). beta8 integrin regulates neurogenesis and neurovascular homeostasis in the adult brain. *J. Cell Sci.* **122**, 1842-1851.
- Mu, Z., Yang, Z., Yu, D., Zhao, Z. and Munger, J. S. (2008). TGFbeta1 and TGFbeta3 are partially redundant effectors in brain vascular morphogenesis. *Mech. Dev.* **125**, 508-516.
- Nguyen, H. L., Lee, Y. J., Shin, J., Lee, E., Park, S. O., McCarty, J. H. and Oh, S. P. (2011). TGF-beta signaling in endothelial cells, but not neuroepithelial cells, is essential for cerebral vascular development. *Lab. Invest.* (in press).
- Nishimura, S. L., Boylen, K. P., Einheber, S., Milner, T. A., Ramos, D. M. and Pytela, R. (1998). Synaptic and glial localization of the integrin alphavbeta8 in mouse and rat brain. *Brain Res.* **791**, 271-282.
- Phng, L. K., Potente, M., Leslie, J. D., Babbage, J., Nyqvist, D., Lobov, I., Ondr, J. K., Rao, S., Lang, R. A., Thurston, G. et al. (2009). Nrarp coordinates endothelial Notch and Wnt signaling to control vessel density in angiogenesis. *Dev. Cell* **16**, 70-82.
- Pitulescu, M. E., Schmidt, I., Benedito, R. and Adams, R. H. (2010). Inducible gene targeting in the neonatal vasculature and analysis of retinal angiogenesis in mice. *Nat. Protoc.* **5**, 1518-1534.
- Proctor, J. M., Zang, K., Wang, D., Wang, R. and Reichardt, L. F. (2005). Vascular development of the brain requires beta8 integrin expression in the neuroepithelium. *J. Neurosci.* **25**, 9940-9948.
- Ramjaun, A. R. and Hodivala-Dilke, K. (2009). The role of cell adhesion pathways in angiogenesis. *Int. J. Biochem. Cell Biol.* **41**, 521-530.
- Reynolds, L. E., Wyder, L., Lively, J. C., Taverna, D., Robinson, S. D., Huang, X., Sheppard, D., Hynes, R. O. and Hodivala-Dilke, K. M. (2002). Enhanced pathological angiogenesis in mice lacking beta3 integrin or beta3 and beta5 integrins. *Nat. Med.* **8**, 27-34.
- Ruhrberg, C., Gerhardt, H., Golding, M., Watson, R., Ioannidou, S., Fujisawa, H., Betsholtz, C. and Shima, D. T. (2002). Spatially restricted

- patterning cues provided by heparin-binding VEGF-A control blood vessel branching morphogenesis. *Genes Dev.* **16**, 2684-2698.
- Scott, A., Powner, M. B., Gandhi, P., Clarkin, C., Gutmann, D. H., Johnson, R. S., Ferrara, N. and Fruttiger, M.** (2010). Astrocyte-derived vascular endothelial growth factor stabilizes vessels in the developing retinal vasculature. *PLoS One* **5**, e11863.
- Silva, R., D'Amico, G., Hodivala-Dilke, K. M. and Reynolds, L. E.** (2008). Integrins: the keys to unlocking angiogenesis. *Arterioscler. Thromb. Vasc. Biol.* **28**, 1703-1713.
- Stenzel, D., Lundkvist, A., Sauvaget, D., Busse, M., Graupera, M., van der Flier, A., Wijelath, E. S., Murray, J., Sobel, M., Costell, M. et al.** (2011). Integrin-dependent and -independent functions of astrocytic fibronectin in retinal angiogenesis. *Development* **138**, 4451-4463.
- Su, H., Kim, H., Pawlikowska, L., Kitamura, H., Shen, F., Cambier, S., Markovics, J., Lawton, M. T., Sidney, S., Bollen, A. W. et al.** (2010). Reduced expression of integrin α v β 8 is associated with brain arteriovenous malformation pathogenesis. *Am. J. Pathol.* **176**, 1018-1027.
- Tchaicha, J. H., Mobley, A. K., Hossain, M. G., Aldape, K. D. and McCarty, J. H.** (2010). A mosaic mouse model of astrocytoma identifies α v β 8 integrin as a negative regulator of tumor angiogenesis. *Oncogene* **29**, 4460-4472.
- Tchaicha, J. H., Reyes, S. B., Shin, J., Hossain, M. G., Lang, F. F. and McCarty, J. H.** (2011). Glioblastoma angiogenesis and tumor cell invasiveness are differentially regulated by β 8 integrin. *Cancer Res.* **71**, 6371-6381.
- Tronche, F., Kellendonk, C., Kretz, O., Gass, P., Anlag, K., Orban, P. C., Bock, R., Klein, R. and Schutz, G.** (1999). Disruption of the glucocorticoid receptor gene in the nervous system results in reduced anxiety. *Nat. Genet.* **23**, 99-103.
- Venstrom, K. and Reichardt, L.** (1995). Beta 8 integrins mediate interactions of chick sensory neurons with laminin-1, collagen IV, and fibronectin. *Mol. Biol. Cell* **6**, 419-431.
- Walshe, T. E., Saint-Geniez, M., Maharaj, A. S., Sekiyama, E., Maldonado, A. E. and D'Amore, P. A.** (2009). TGF-beta is required for vascular barrier function, endothelial survival and homeostasis of the adult microvasculature. *PLoS One* **4**, e5149.
- Watson, A. R., Pitchford, S. C., Reynolds, L. E., Direkze, N., Brittan, M., Alison, M. R., Rankin, S., Wright, N. A. and Hodivala-Dilke, K. M.** (2010). Deficiency of bone marrow beta3-integrin enhances non-functional neovascularization. *J. Pathol.* **220**, 435-445.
- Worthington, J. J., Klementowicz, J. E. and Travis, M. A.** (2010). TGFbeta: a sleeping giant awoken by integrins. *Trends Biochem. Sci.* **36**, 47-54.
- Wu, M. Y. and Hill, C. S.** (2009). Tgf-beta superfamily signaling in embryonic development and homeostasis. *Dev. Cell* **16**, 329-343.
- Xu, Q., Wang, Y., Dabdoub, A., Smallwood, P. M., Williams, J., Woods, C., Kelley, M. W., Jiang, L., Tasman, W., Zhang, K. et al.** (2004). Vascular development in the retina and inner ear: control by Norrin and Frizzled-4, a high-affinity ligand-receptor pair. *Cell* **116**, 883-895.
- Yafai, Y., Lange, J., Wiedemann, P., Reichenbach, A. and Eichler, W.** (2007). Pigment epithelium-derived factor acts as an opponent of growth-stimulatory factors in retinal glial-endothelial cell interactions. *Glia* **55**, 642-651.
- Ye, X., Wang, Y., Cahill, H., Yu, M., Badea, T. C., Smallwood, P. M., Peachey, N. S. and Nathans, J.** (2009). Norrin, frizzled-4, and Lrp5 signaling in endothelial cells controls a genetic program for retinal vascularization. *Cell* **139**, 285-298.
- Zhang, Y. and Barres, B. A.** (2010). Astrocyte heterogeneity: an underappreciated topic in neurobiology. *Curr. Opin. Neurobiol.* **20**, 588-594.
- Zhu, J., Motejlek, K., Wang, D., Zang, K., Schmidt, A. and Reichardt, L. F.** (2002). beta8 integrins are required for vascular morphogenesis in mouse embryos. *Development* **129**, 2891-2903.